



Figures and figure supplements

Intracellular uptake of macromolecules by brain lymphatic endothelial cells during zebrafish embryonic development

Max van Lessen et al

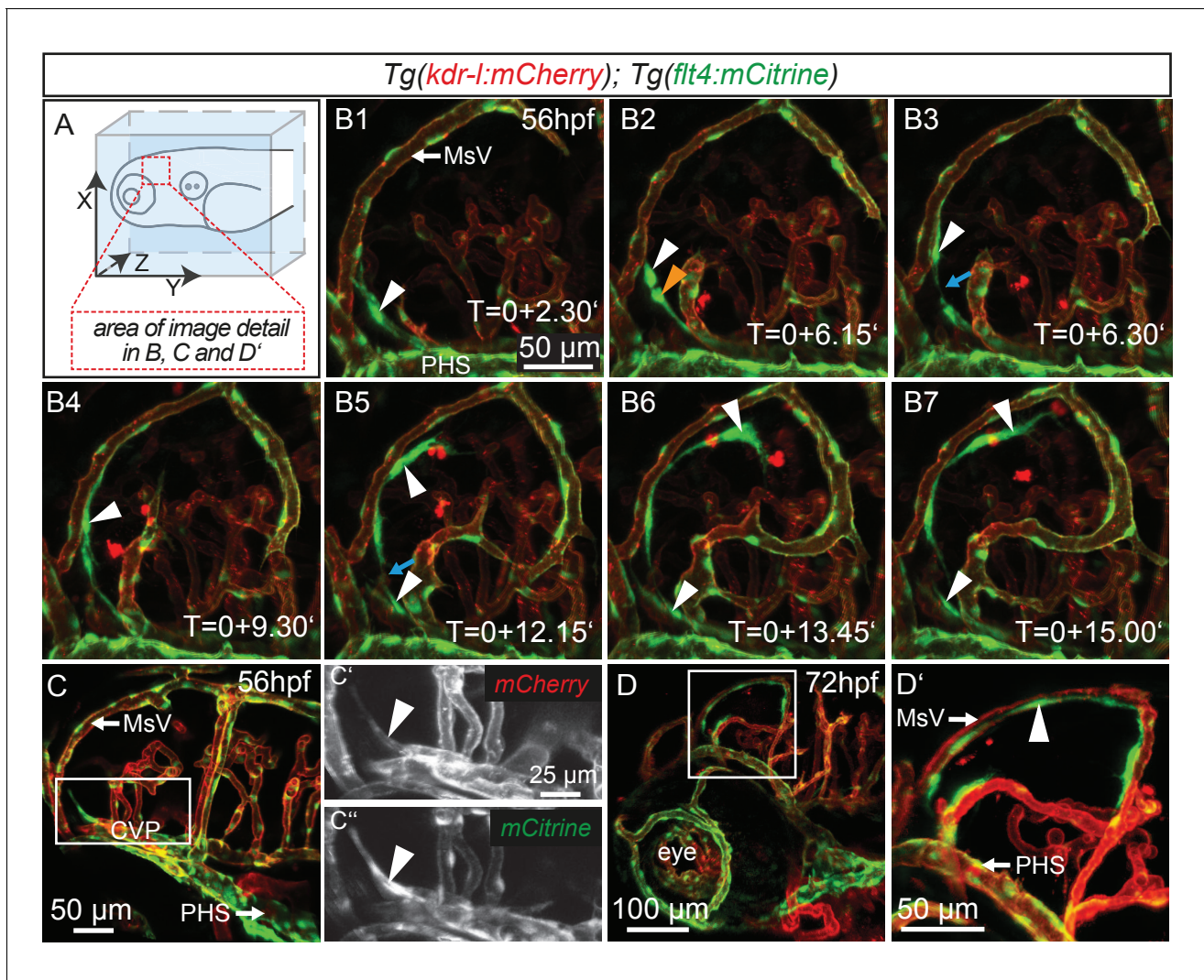


Figure 1. *flt4* positive cells sprout from the choroidal vascular plexus and migrate along blood vessels. In all images blood vessels are highlighted in red (*kdr-l:mCherry*) and lympho-venous cells in green (*flt4:mCitrine*). (A) Overview and orientation of zebrafish embryos imaged in B–D. (B1 – B7) Time-lapse still images of lateral confocal projections of the TeO. At 56hpf strong mCitrine positive but low mCherry expressing ECs sprout from a vessel behind the PHS and migrate along the MsV (white arrow). Following initial sprouting the cell divides (B2, white and orange arrowheads). Leading and following cells appear to temporarily lose contact (B3 and B5, blue arrow). After making contact to the MsV the sprout continues migration (B4–B7). (C) Partial projection of the sprouting cells (cropping of the PHS) reveals that the migrating cells originate from the more proximal positioned CVP at around 56hpf. Sprouting cells express low mCherry but high mCitrine levels compared to the CVP (inset C'–C''). (D) Lateral confocal projection of the head region shows that at 72hpf *flt4* positive ECs (white arrowheads) form a loop aligned next to the MsVs (white arrowheads). (D') Higher magnification of the boxed area in (D). Data are representative of at least five independent experiments. CVP, choroidal vascular plexus; EC, endothelial cell; hpf, hours post fertilization; MsV, mesencephalic vein; PHS, primary head sinus; TeO, Optic Tectum. Apostrophe in B1–B7 denotes hours.

DOI: [10.7554/eLife.25932.002](https://doi.org/10.7554/eLife.25932.002)

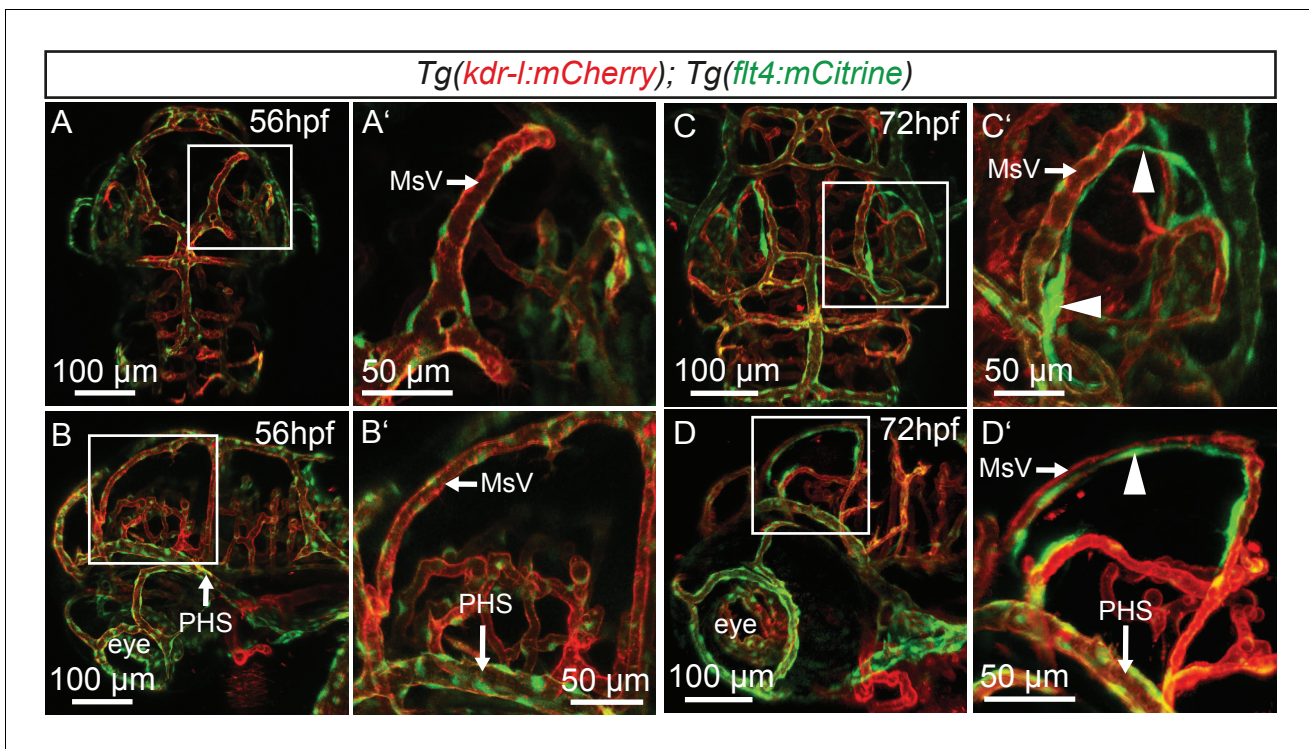


Figure 1—figure supplement 1. *flt4* positive cells develop between 56 and 72 hpf. In all images blood vessels are highlighted in red (*kdr-l:mCherry*) and lympho-venous cells in green (*flt4:mCitrine*). (A–D) Representative dorsal and lateral confocal projection of the zebrafish head region. Until 56 hpf there are no apparent *flt4* positive, *kdr-l* negative cells visible (dorsal view in A, lateral view in B). In 3dpf embryos, a bilateral loop of loosely connected *flt4* positive, *kdr-l* negative cells has formed next to the MsV (dorsal view in C, lateral view in D, white arrowheads). Data are representative of at least three independent experiments. hpf, hours post fertilization; MsV, mesencephalic vein; PHS, primary head sinus.

DOI: [10.7554/eLife.25932.003](https://doi.org/10.7554/eLife.25932.003)

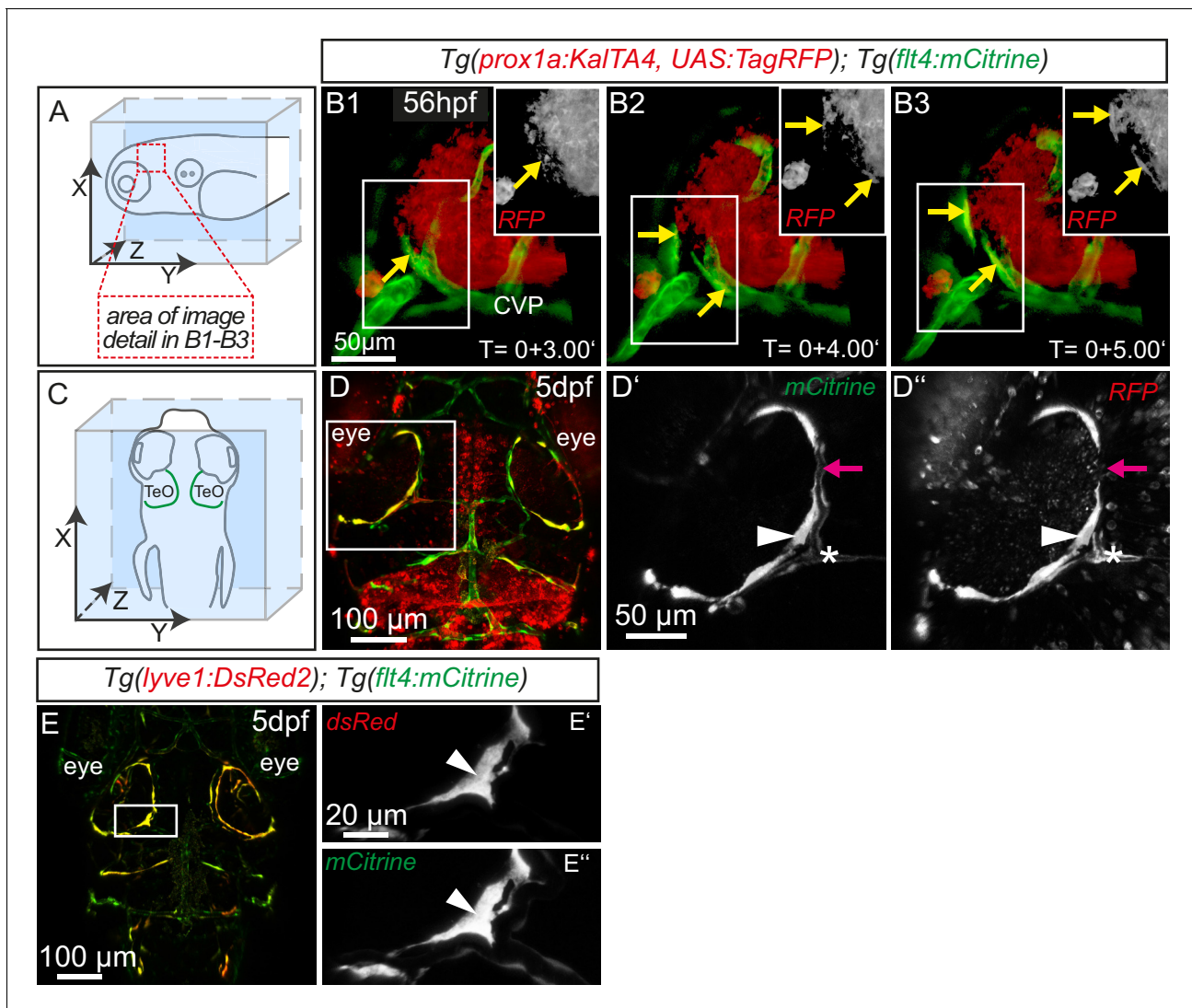


Figure 2. Sprouting *flt4* positive endothelial cells express *prox1a* and *lyve1*. (A) and (C) Overview and orientation of 56hpf and 5dpf zebrafish embryos shown in B1-B3 (A) and D-E'' (C). Green lines in C illustrate the position of mCitrine positive ECs. (B1-B3) Time-lapse still images of partial lateral confocal projections of the TeO as depicted in A (red inset). At 56hpf tagRFP indicates *prox1a* promoter activity in mCitrine positive endothelial sprouts (yellow arrows). Note that the RFP positive red cell mass above the CVP likely reports *prox1a* expression in cranial ganglia within the TeO. (D) Strong *prox1a* promoter activity persists in the mCitrine positive loop structure (inset, white arrowhead) but is absent in neighboring MsV (inset, pink arrow) at 5dpf. Note also tagRFP expression around a small part of the MsV (inset, white asterisk). (E) *flt4* positive ECs express *lyve1* at 5dpf (E',E'' inset, white arrowhead). Data are representative of at least three independent experiments. CVP, choroidal vascular plexus; dpf, days post fertilization; hpf, hours post fertilization; MsV, mesencephalic vein; TeO, Optic Tectum. Apostrophe in B1-B3 denotes hours.

DOI: [10.7554/eLife.25932.005](https://doi.org/10.7554/eLife.25932.005)

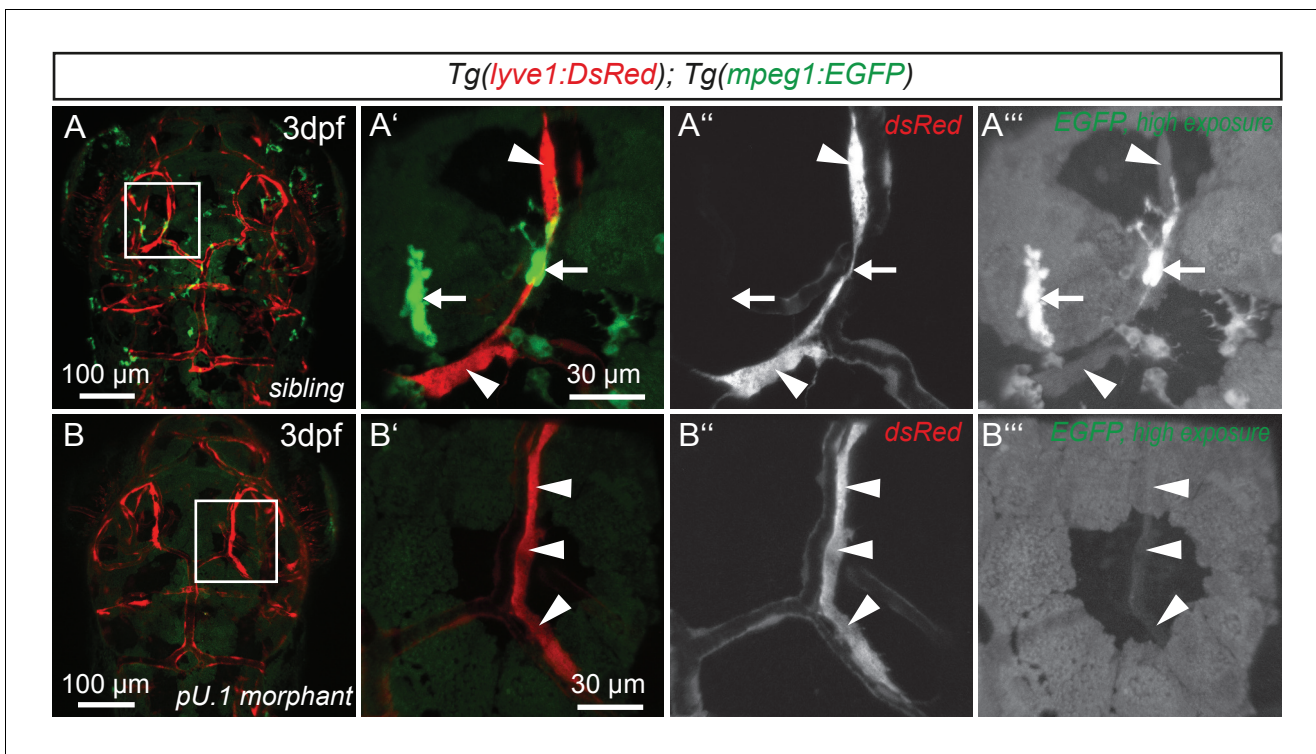


Figure 3. *flt4* positive cells are not of myelopoietic origin. (A) and (B) Dorsal view of partial confocal projections of 3dpf double transgenic *Tg(lyve1:DsRed)^{nz101}; Tg(mpeg1:EGFP)^{gl22}* embryos. Brain resident macrophages strongly express *mpeg1:EGFP* (A'–A''', white arrows) while *lyve1* positive LECs are only weakly *EGFP* positive (A'–A''', white arrowheads) in uninjected control embryos. Depletion of the myelopoietic lineage by injection of *pU.1* (*spi1b*) morpholinos ablates all *EGFP* positive macrophages but does not affect the formation of *lyve1* positive LECs (B'–B''', white arrowheads). dpf, days post fertilization; LEC, lymphatic endothelial cell.

DOI: [10.7554/eLife.25932.006](https://doi.org/10.7554/eLife.25932.006)

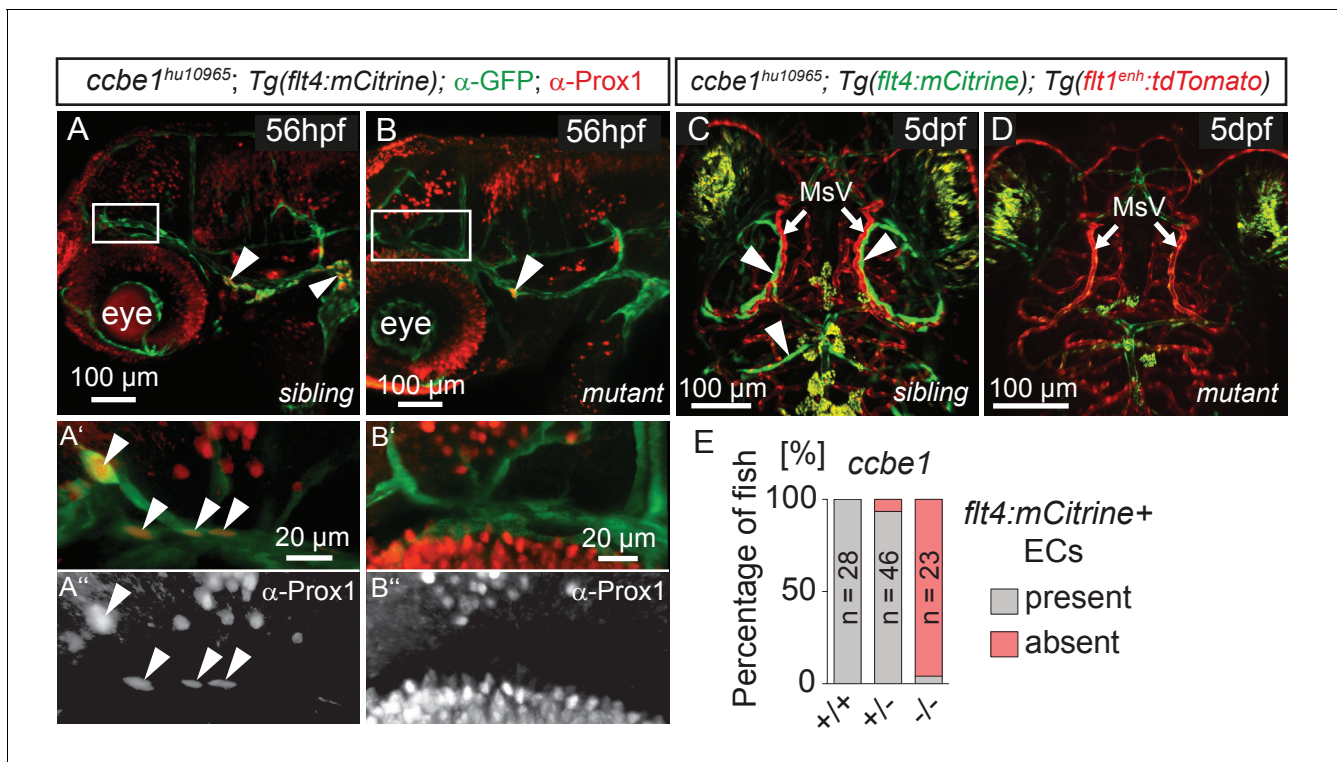


Figure 4. *flt4* positive cells are sensitive to ablation of the *vegfc/ccbe1* pathway. (A) and (B) Antibody staining detects Prox1 protein in the GFP positive CVP and sprouting ECs in wild type sibling (A) but not in *ccbe1* mutant (B) embryos (A',A'' insets, white arrowheads). Note few Prox1 expressing cells remaining in mutants at the site of facial lymphatic sprouting (B, white arrowhead). (C) and (D) Absence of *flt4:mCitrine* expressing ECs in *ccbe1* mutant (D) but not in sibling controls (C, white arrowheads) in 5dpf embryos. *Tg(flt1^{enh}:tdTomato)* labels arteries. (E) Quantification of results shown in C and D. Data are representative of at least two independent experiments. CVP, choroidal vascular plexus; dpf, days post fertilization; EC, endothelial cell; hpf, hours post fertilization; MsV, mesencephalic vein; +/+, wildtype; +/-, heterozygous; -/-, mutant.

DOI: 10.7554/eLife.25932.007

The following source data is available for figure 4:

Source data 1. Zebrafish embryos from an incross of *Tg(flt1^{enh}:tdTomato)*; *Tg(flt4:mCitrine)* heterozygous for the mutant *ccbe1^{hu10965}* allele were analyzed by fluorescent stereomicroscopy at 5dpf for the presence or absence of *flt4:mCitrine* expressing ECs in the head (as depicted in **Figure 4C and D**).

DOI: 10.7554/eLife.25932.008

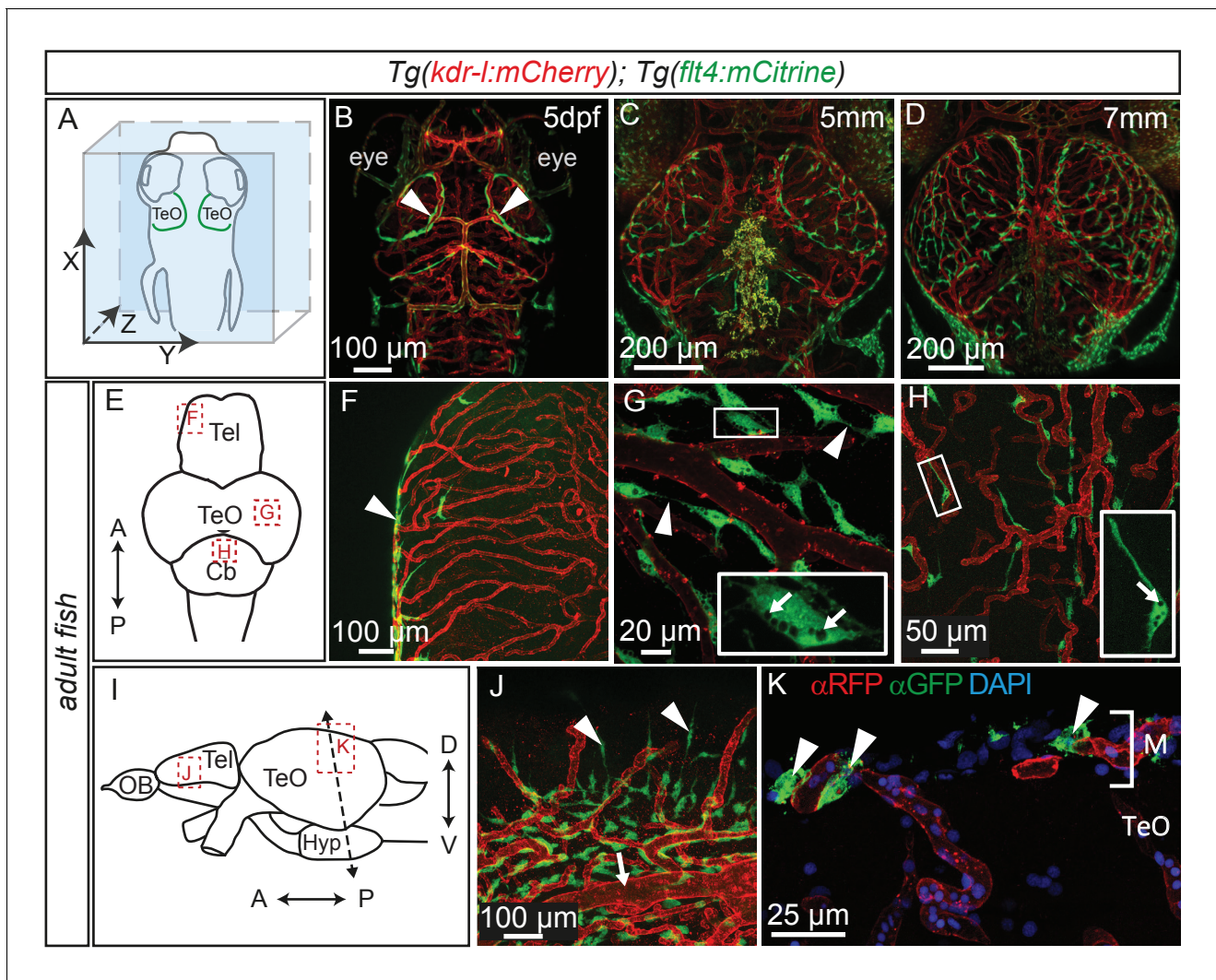


Figure 5. Perivascular position of *flt4* positive BLECs in larval stages and adult meninges. (A) Overview and orientation of zebrafish embryos imaged in B–D. (B) Dorsal confocal projections of the head region show that at 5dpf *flt4* positive BLECs (white arrowheads) form a bilateral loop in the TeO which aligns next to the MsVs (white arrowheads). (C) and (D) Dorsal confocal projections at 5 mm and 7 mm stages show increasing spreading of *flt4* positive ECs, particularly over the TeO. (E) Schematic diagram (dorsal view) of adult brain. Dotted boxes show area of image detail of F–H. (F) The dorsal surface of the Tel displays a distinct absence of *flt4:mCitrine* positive cells. (G) and (H) A dorsal view of the TeO and Cb, respectively, shows *flt4:mCitrine* positive BLECs (green) closely associated with surface *kdr-l:mCherry* positive blood vasculature (red), interacting with vessels and one another via thin processes (white arrowheads). BLECs contain multiple internal compartments (inset, white arrows). BLECs on the cerebellar surface are less dense and are morphologically distinct, exhibiting an elongated shape (inset). (I) Schematic diagram (lateral view) of adult brain. Dotted boxes show area of image detail of J and K, and the dotted line shows the section plane in K. (J) BLECs on the lower half of the lateral telencephalic midline boundary cluster around smaller vessels branching off from the anterior cerebral carotid artery at the lateral midline of the telencephalon (white arrow) with a few cells sending sparse and elongated processes towards the dorsal surface (white arrowheads). (K) Coronal section of the adult brain shows *flt4:mCitrine* positive BLECs (green) (white arrowheads) closely associated with *kdr-l:mCherry* positive vasculature (red) exclusively within the meninges (M) but not along the vessels extending ventrally into the tectal neuropil. DAPI nuclear counter stain (blue). Data are representative of at least three independent experiments. BLEC, brain lymphatic endothelial cell; Cb, Cerebellum; dpf, days post fertilization; EC, endothelial cell; Hyp, hypothalamus; M, Meninges; MsV, mesencephalic vein; Tel, Telencephalon; TeO, Optic Tectum.

DOI: 10.7554/eLife.25932.009

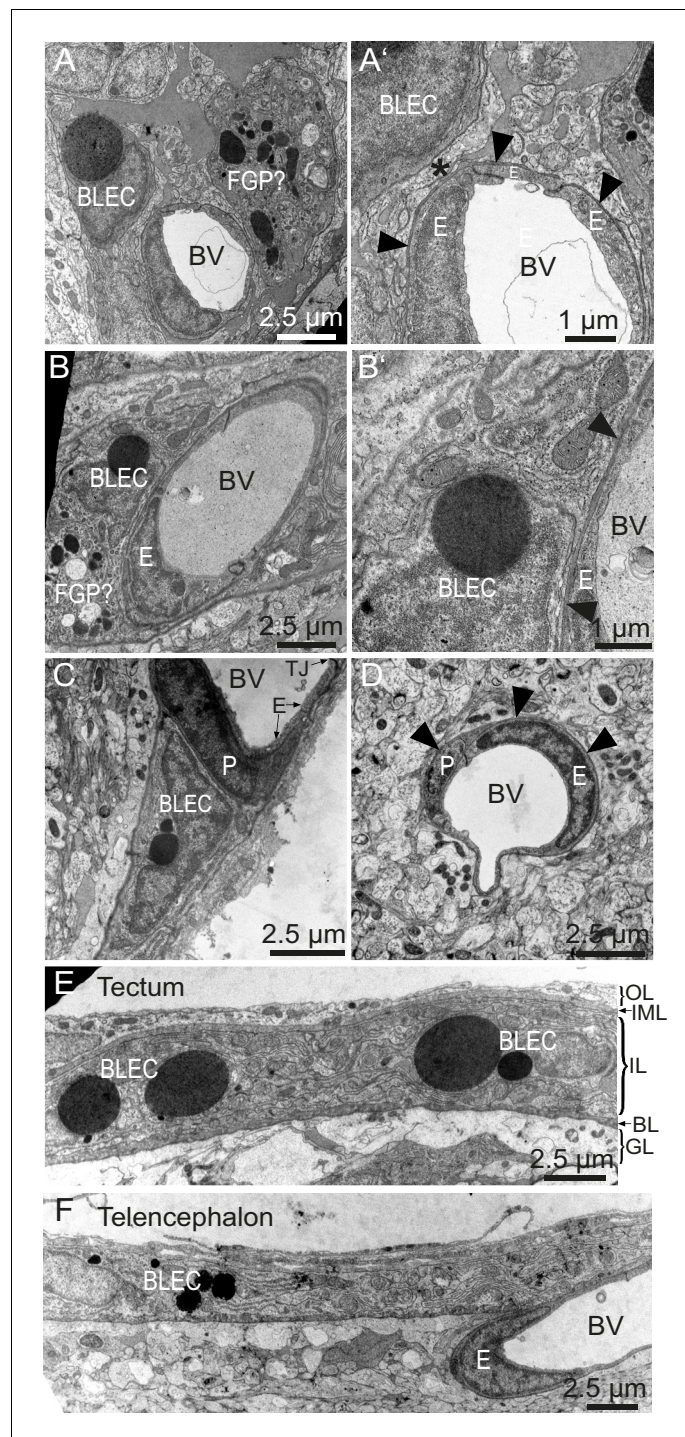


Figure 6. BLEC ultrastructure revealed in TEM of adult brain meninges. (A) and (B) TEM micrographs of tangential sections of the domed tectal surface revealed cells (BLEC) with large spherical inclusions in proximity to meningeal blood vessels (BV). Higher magnification shows that BLECs are not contained within the basement membrane (A' and B', arrowheads) of endothelial cells (E) and are separated from the vessels by other cellular processes (e.g. asterisk in A'). Putative Mato/FGP cells are indicated (FGP?). (C) and (D) Pericytes (P) maintain close contact with endothelial cells (E) and are found under the basement membrane (arrowheads). BLECs are only found in the meninges (C) and are absent near blood vessels in the neuropil (D) of the brain. (E) and (F) T/S sections of tectal (E) and latero-ventral telencephalic (F) meninges showing BLECs are present in the inner layer (IL) of the meningeal covering. BLEC, brain lymphatic endothelial cell; E, endothelial cell; FGP, fluorescent granular
Figure 6 continued on next page

Figure 6 continued

perithelial cell; P, pericyte; TJ, tight junction. Nomenclature of meningeal layers according to **Momose et al. (1988)**: OL, outer layer; IML, intermediate layer; IL, inner layer, BL, basal lamina; GL, glia limitans.

DOI: [10.7554/eLife.25932.012](https://doi.org/10.7554/eLife.25932.012)

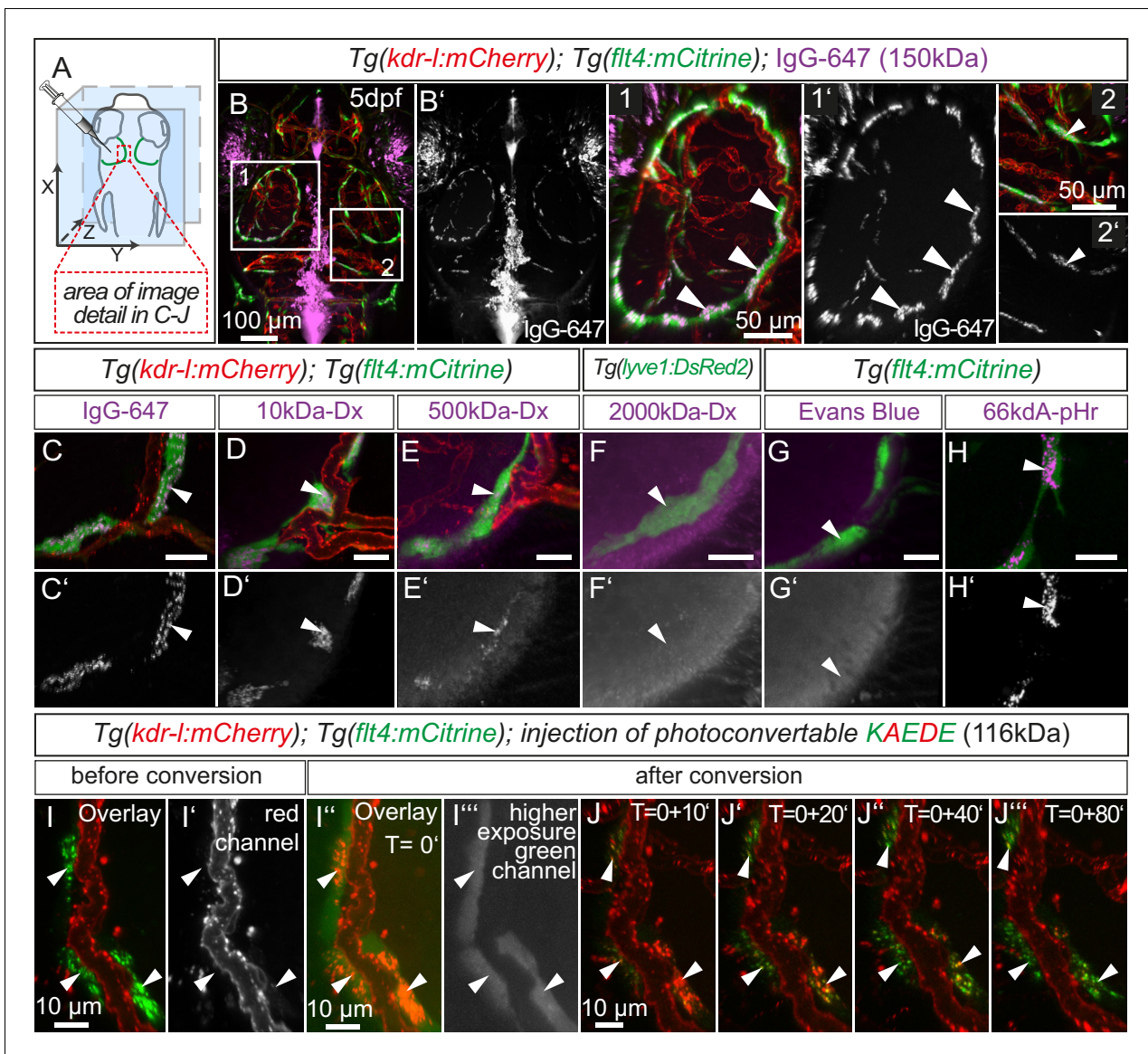


Figure 7. BLECs dynamically take up macromolecules. (A) Overview of the zebrafish head region and intratectal injection site of fluorescent dyes into the center of the TeO close to the meninges. Red inset denotes area of image detail in C–J. (B–J) Representative dorsal confocal projection of 5dpf embryos injected with different tracer dyes as indicated. Injected IgG-647, 10kDa-Dx, 500kDa-Dx and 66kDa-pHr specifically localize to vesicles in mCitrine positive BLECs but not to mCherry positive blood vessels (B–E, H, I and J, white arrowheads). BLECs do not accumulate high MW dextran or Evans Blue (F and G, white arrowhead). BLECs strongly label with the pH-sensitive dye pHrodo (pHr) indicating tracer internalization (H, white arrowhead). (I) and (J) Injected KAEDE protein is taken up by BLECs (I and I', white arrowheads) and can be photoconverted to red by localized UV-exposure to a region of interest (I'' and I''', white arrowheads). 10 min after photoconversion, the amount of converted red KAEDE decreases dramatically (J) and the signal is almost completely lost after 80 min (J''', white arrowheads). In the same time course photoconverted BLECs re-accumulate non-converted green KAEDE protein (J''', white arrowheads). Scale bar in C–H corresponds to 20 μ m. Data are representative of at least two independent experiments. BLEC, brain lymphatic endothelial cell; dpf, days post fertilization; Dx, Dextran; IgG-647, IgG-conjugated Alexa Fluor 674; TeO, Optic Tectum; pHr, pHrodo Red Avidin. Apostrophe in J denotes minutes.

DOI: 10.7554/eLife.25932.013

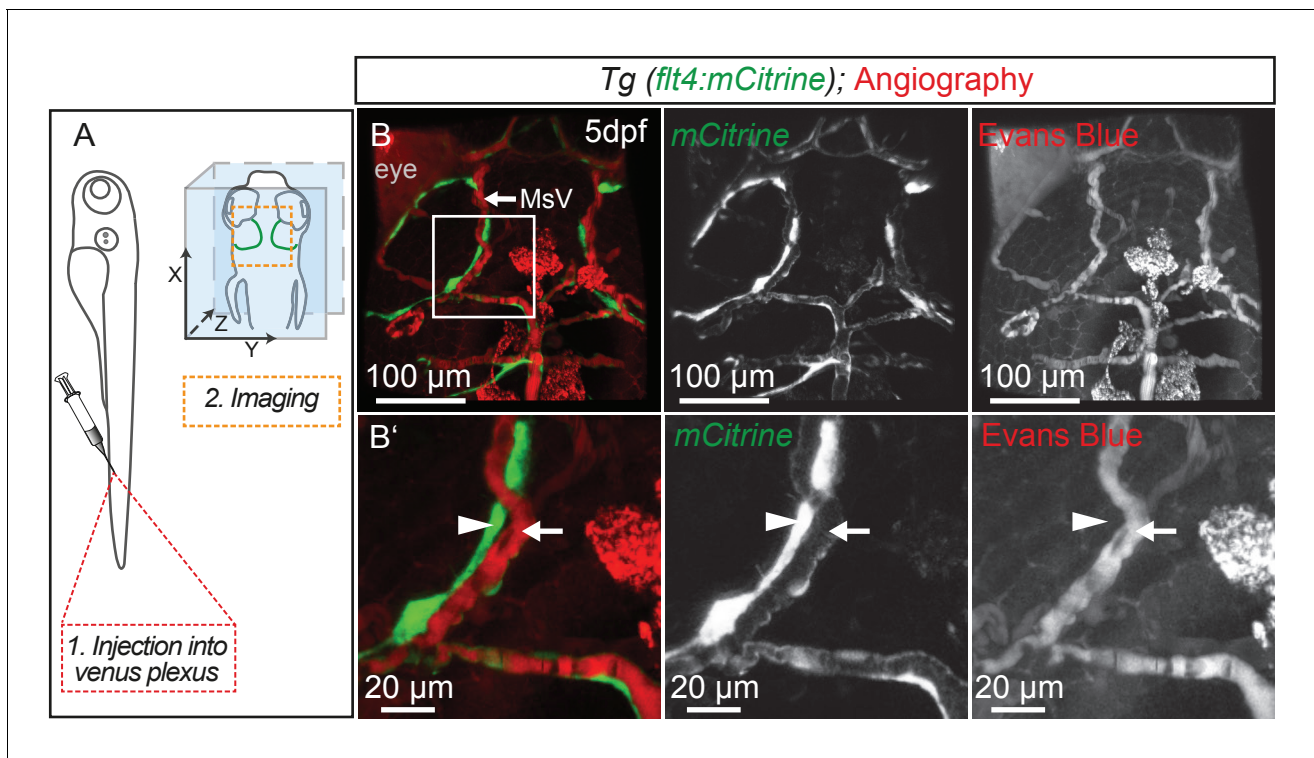


Figure 7—figure supplement 1. BLECs do not carry blood flow. (A) Overview of the injection site for angiography into the venous plexus and of the region used for imaging (orange broken box) in the zebrafish head shown in B. (B) Representative dorsal confocal projection of 5dpf embryos with lympho-venous cells in green (*flt4:mCitrine*). Injected Evans Blue (red fluorescence) is confined to blood vessels (white arrow) and is not taken up by BLECs (white arrowheads). Data are representative of at least two independent experiments. BLEC, brain lymphatic endothelial cell; dpf, days post fertilization; MsV, mesencephalic vein.

DOI: [10.7554/eLife.25932.014](https://doi.org/10.7554/eLife.25932.014)

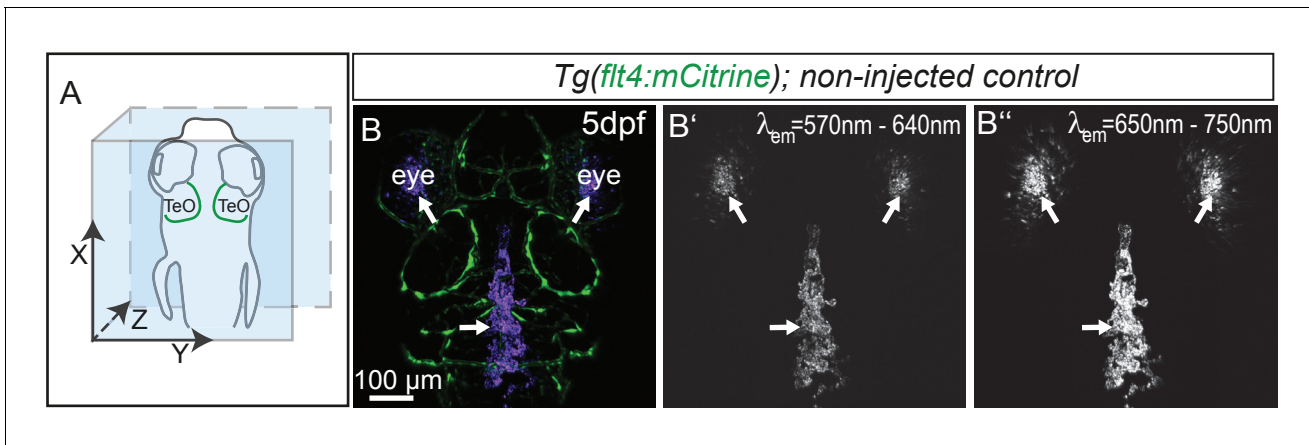


Figure 7—figure supplement 2. Eyes and skin pigmentation is autofluorescent in non-injected embryos. (A) Orientation of the zebrafish head imaged in B. (B) Representative dorsal confocal projection of non-injected 5dpf *Tg(flt4:mCitrine)* embryos marking lympho-venous cells in green. Excitation at 568 nm (B') and 647 nm (B'') shows auto-fluorescent signal from the eyes and skin pigmentation within the emission spectra of red and near-infrared fluorophores (B' and B'', white arrowheads). Data are representative of at least two independent experiments. dpf, days post fertilization; MsV, mesencephalic vein; TeO, Optic Tectum.
DOI: [10.7554/eLife.25932.015](https://doi.org/10.7554/eLife.25932.015)

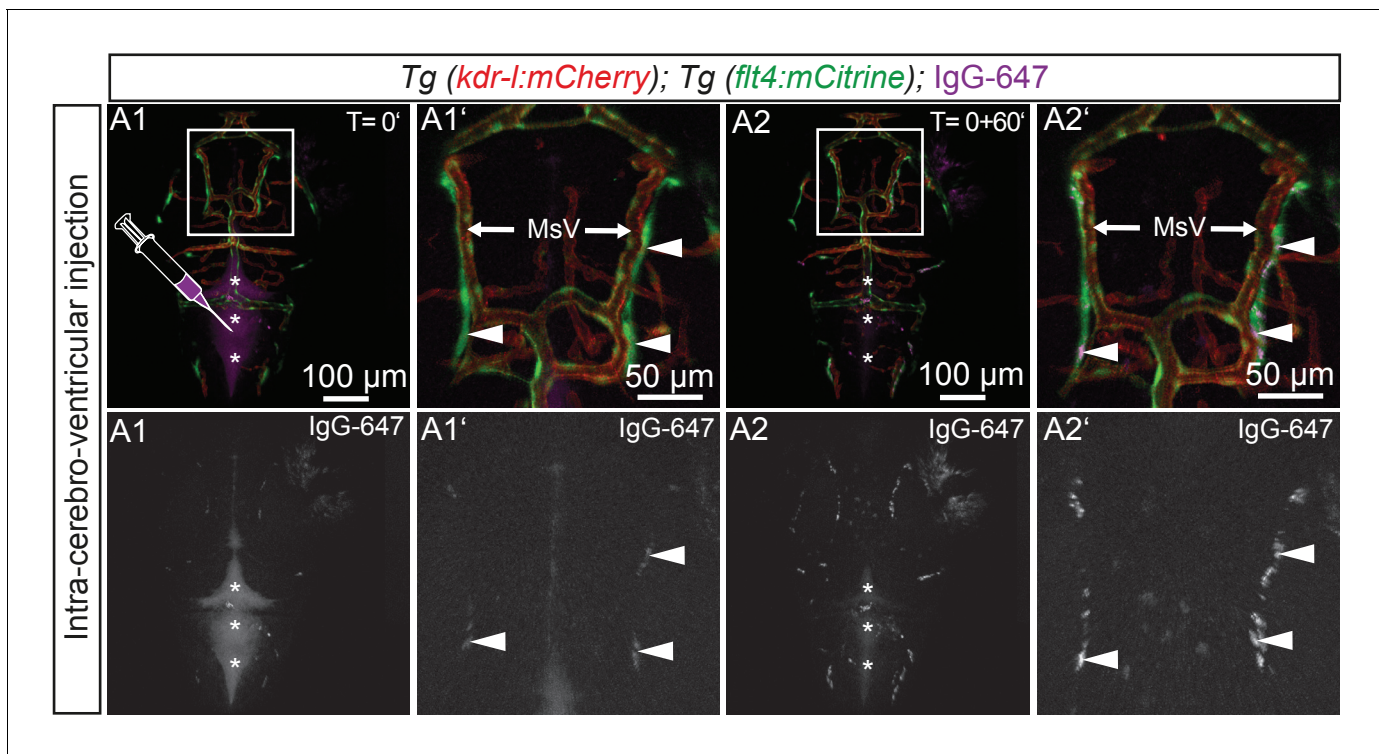


Figure 7—figure supplement 3. BLECs take up tracer from ventricles. Blood vessels are highlighted in red (*kdr-l:mCherry*) and lympho-venous cells in green (*flt4:mCitrine*). IgG-647 is pseudo-colored in purple. (A1–A2) Time-lapse still images of representative dorsal confocal projection of 72hpf embryo injected with IgG-647 into the hindbrain ventricle. Immediately after injection, the tracer dye is confined to the hind- and midbrain ventricle (A1, asterisks) and only very faint signal is detected from *flt4* positive *kdr-l* negative BLECs (A1, inset, white arrowheads). Within 60 min, the tracer cleared from the ventricular space (B1, asterisks) and accumulated at BLECs (A2, inset, white arrowheads). Data are representative of at least two independent experiments. BLEC, brain lymphatic endothelial cell; hpf, hours post fertilization; IgG-647, IgG-conjugated Alexa Fluor 647; MsV, mesencephalic vein.

DOI: [10.7554/eLife.25932.016](https://doi.org/10.7554/eLife.25932.016)

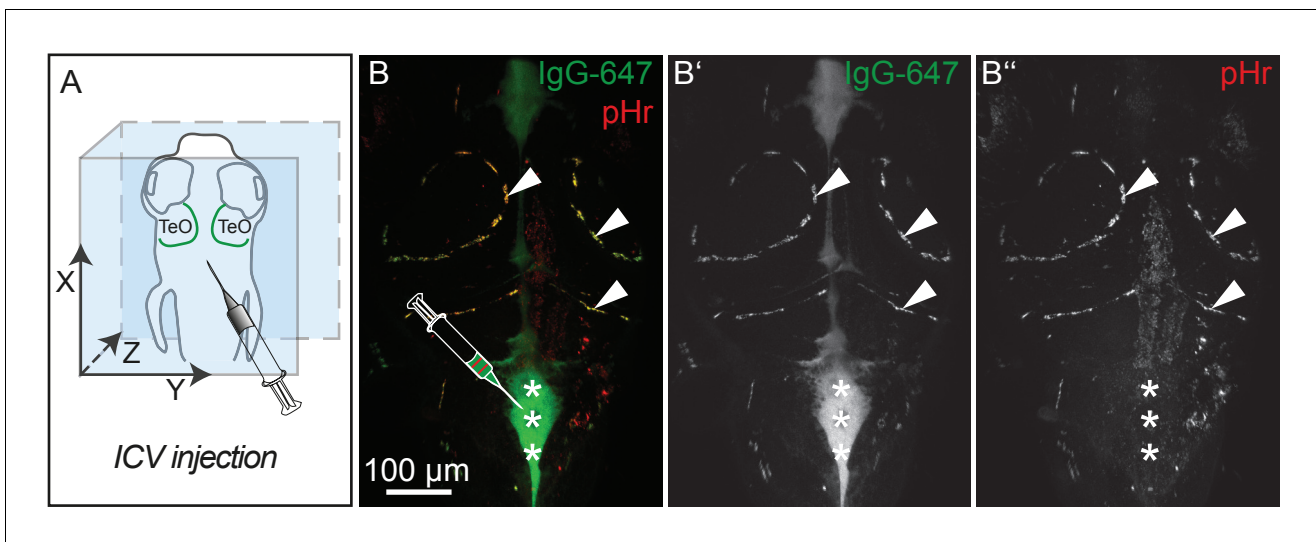


Figure 7—figure supplement 4. pH-sensitive pHrodo Red Avidin fluoresces more brightly after uptake into BLECs. (A) Orientation of the zebrafish head and injection site of fluorescent dyes into the hindbrain ventricle of a 5dpf embryo as shown in B. (B) Representative dorsal confocal projection of 5dpf embryos injected with both IgG-647 and pHr. Injected IgG-647 is clearly visible in both the ventricles (asterisks) and BLECs (arrowheads), while pHr predominantly fluoresces within BLECs, probably reflecting localization to low pH compartments (B–B'', asterisks and arrowheads). Data are representative of at least five independent experiments. BLEC, brain lymphatic endothelial cell; dpf, days post fertilization; ICV, intra-cerebro-ventricular; IgG-647, IgG-conjugated Alexa Fluor 647; TeO, Optic Tectum; pHr, pHrodo Red Avidin.

DOI: [10.7554/eLife.25932.017](https://doi.org/10.7554/eLife.25932.017)

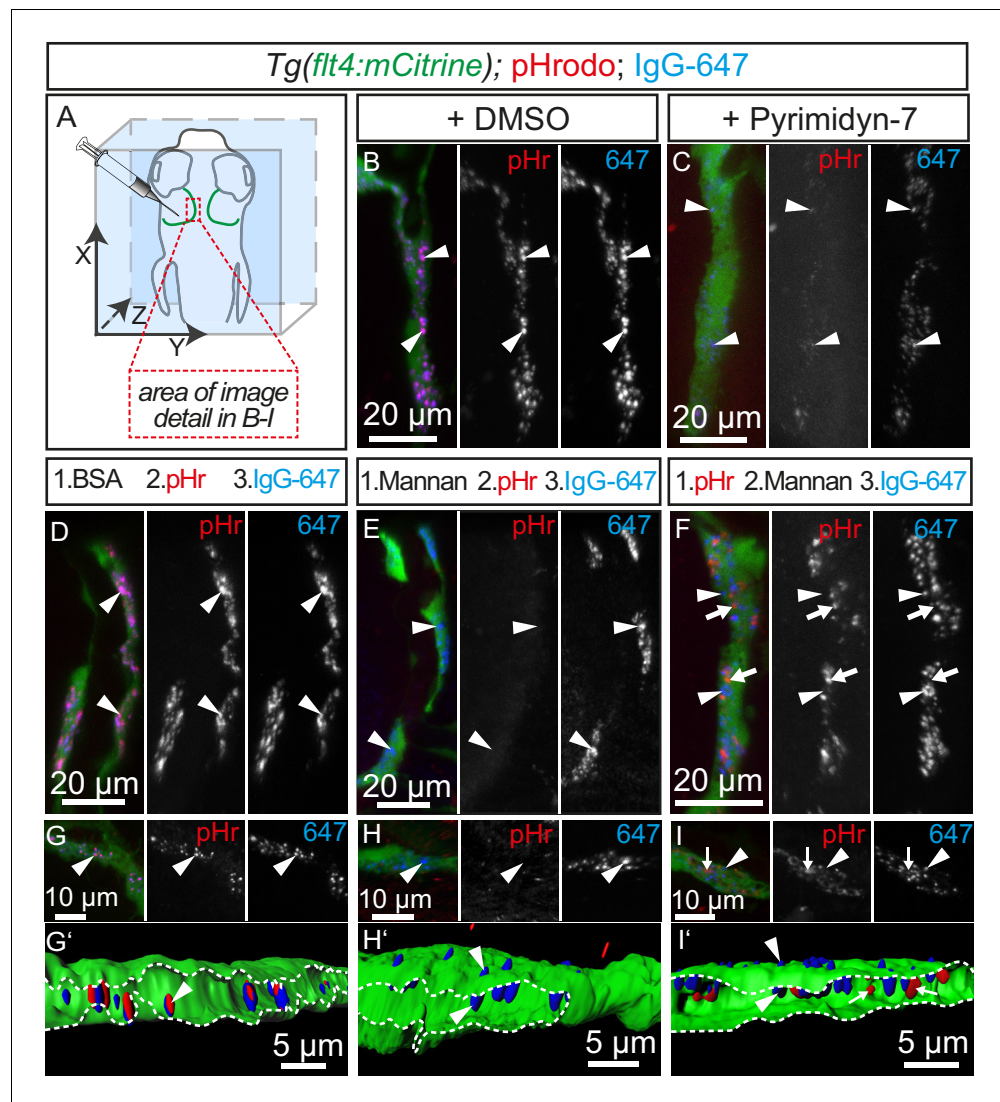


Figure 8. Tracer uptake by BLECs is inhibited by mannan administration. (A) Overview of the zebrafish head region depicting intratectal injection of fluorescent dyes into the center of the TeO close to the meninges in 5dpf embryos. Red inset denotes area of image detail for representative dorsal confocal projections in B–I. (B) and (C) In DMSO treated fish co-injection of pHr and IgG-647 reveals high degree co-localization of both tracers in vesicles within mCitrine positive BLECs (B, white arrowheads). Inhibition of dynamin-dependent endocytosis with Pyrimidin-7 results in reduced signal intensity from IgG-647 positive vesicles and an almost complete block of pHr uptake (C, white arrowheads). (D–F) Separate, consecutive injections of BSA or mannan with pHr and IgG-647. Injection of BSA, pHr and IgG-647 results in co-localization of both tracers in BLECs (D, white arrowheads). In contrast, initial injection of mannan completely blocks the uptake of pHr but not the accumulation of IgG-647 to BLECs (E, white arrowheads). However, initial injection of pHr followed by mannan and IgG-647 results in accumulation of both tracers in BLECs with hardly any co-localization (F, white arrowheads and arrows). (G–I) Same experimental setup as in D–F except the embryos were fixed in PFA five minutes after the last injection to enable higher resolution imaging. Area within the white dotted lines in 3D-reconstructions reveals the lumen of BLECs (G', H' and I'). In BSA control injected fish both dyes co-localize in intraluminal vesicles (G and G', white arrowheads). In mannan injected fish, IgG-647 cannot be internalized completely but remains stuck at the cell surface, (H and H', white arrowheads). Finally, initial injection of pHr reveals internalized vesicular pHr and membrane associated IgG-647 (I and I', white arrows and white arrowheads). Data are representative of at least two independent experiments. BLEC, brain lymphatic endothelial cell; BSA, bovine serum albumin; dpf, days post fertilization; IgG-647, IgG-conjugated Alexa Fluor 647; PFA, paraformaldehyde; pHr, pHrodo Red Avidin; TeO, Optic Tectum.

DOI: [10.7554/eLife.25932.021](https://doi.org/10.7554/eLife.25932.021)

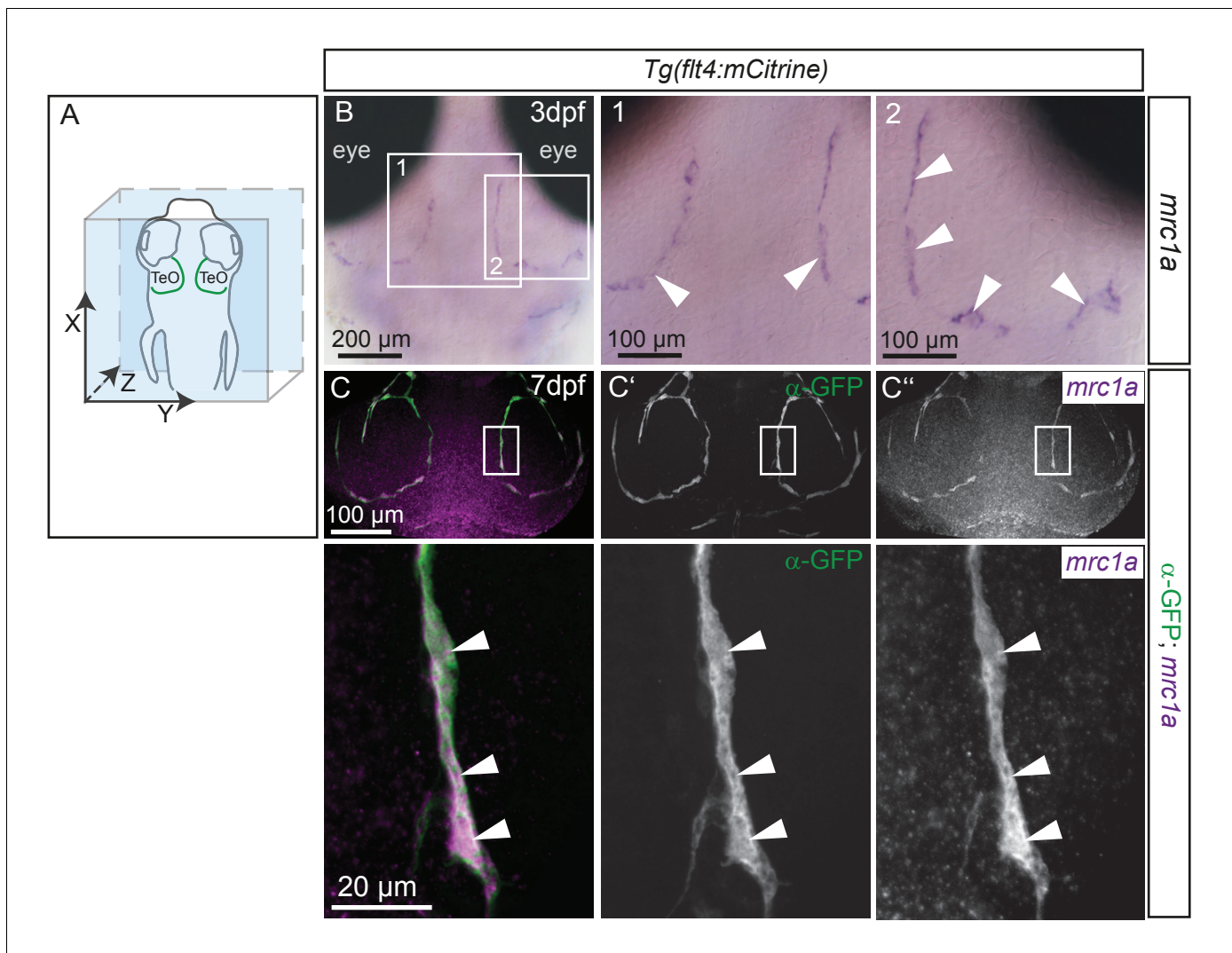


Figure 8—figure supplement 1. BLECs express *mrc1a*. (A) Overview and orientation of zebrafish embryo imaged in B and C, with the arrangement of BLECs over the brain illustrated by the green lines. (B) In situ hybridization in 80hpf zebrafish embryos reveals *mrc1a* mRNA expression in BLECs (white arrowheads in insets 1 and 2). Note discontinuous staining pattern suggesting labeling of individual, loosely connected cells. (C) Double fluorescent in situ shows *mrc1a* mRNA (purple) expression persists in 7dpf embryos and specifically localizes to mCitrine expressing BLECs labelled with α -GFP antibody (green) (white arrowheads in insets). Data are representative of three independent experiments. BLEC, brain lymphatic endothelial cell; TeO, Optic Tectum.

DOI: [10.7554/eLife.25932.022](https://doi.org/10.7554/eLife.25932.022)

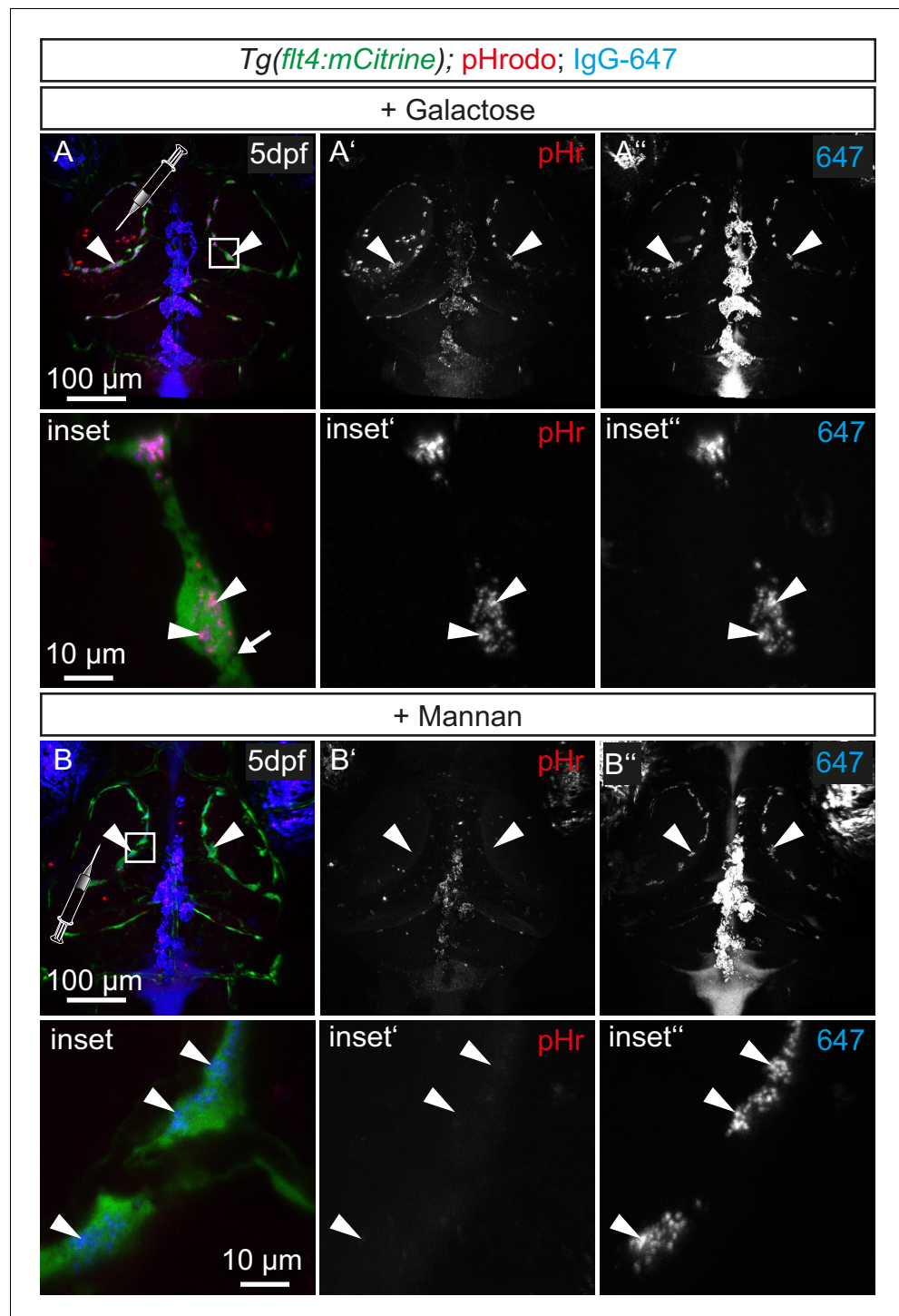


Figure 8—figure supplement 2. Tracer uptake by BLECs is not inhibited by galactose administration. (A) and (B) Representative dorsal confocal projections of the zebrafish head region depicting intratretal injection of galactose (A) or mannan (B) prior to injection of fluorescent dyes into the center of TeO close to the meninges in 5dpf *Tg(flt4:mCitrine)* embryos. After injection of the monosaccharide galactose, *flt4* positive BLECs still endocytose both pHr and IgG-647 (A, white arrowheads). In contrast, mannan administration blocks dye uptake indicated by the absence pHr positive vesicles in BLECs (B), while 647 can still bind to the PM (B, white arrowheads). BLEC, brain lymphatic endothelial cell; dpf, days post fertilization; IgG-647, IgG-conjugated Alexa Fluor 674; pHr, pHrodo Red Avidin; TeO, Optic Tectum.

DOI: [10.7554/eLife.25932.023](https://doi.org/10.7554/eLife.25932.023)